Design of tunable gold metasurface refractive index biosensor using $Ge_2Sb_2Te_5$ material

S. SYED MUSTHAFA GANI[1,*], S. ARUN PRAKASH[2], SHOBHIT K. PATEL[3,4]

[1]*Department of EEE, Mohamed Sathak Engineering College, Kilakarai-623806, Tamil Nadu, India*
[2]*Department of EEE,University College of Engineering, Ramanathapuram-623513, Tamil Nadu, India*
[3]*Department of Electronics and Communication Engineering, Marwadi University, Gujarat, Rajkot, 360003, India*
[4]*Department of Computer Engineering, Marwadi Unversity, Gujarat, Rajkot, 360003, India*

We present a tunable gold metasurface refractive index biosensor. The tunability is achieved by two different phases of $Ge_2Sb_2Te_5$ (GST) material. The sensitivity of refractive index sensor is also enhanced by this GST material based metasurface biosensor design. The results in the form of absorption, electric field, and magnetic field are presented. The design is also observed for different geometrical parameter variations. The incident angle is also varied to observe its effect on absorption of the design. The crystalline phase of GST materials is giving better sensitivity compared to amorphous phase of GST. The proposed design results are compared with previously published design results. The comparison clearly shows that proposed design has better sensitivity compared to other designs. The proposed biosensor can become a building block for medical sensing devices.

1. Introduction

Biosensor plays a vital role not only in medical diagnosis but it is also used in environmental monitoring, forensic research, etc., [1]. The biosensor senses the biomolecules or analyteswhich are placed on its surface. The sensing gives the result in the form of different parameters based on the biomolecules it is sensing [2]. The optical biosensor is one of the main biosensors used nowadays. There are main two types of optical biosensors. The first type is labeled biosensor and second type is label-free biosensor [3]. Lable-free method act as a primary source that givesa direct signal of molecule binding with each other without the involvement of secondary measurements such as labels. They are used for the screening purpose of biomolecules in a research laboratory. Their classifications are divided on basis of their group type. They enable real-time monitoring of the biomolecule that helps in the recognition [4]. The label-free method is used in this research because it gives the suitability for detection of biomolecules that are not even labelled. The label-free method is better for detecting analytesthatare not easy to label. Their detection also removes many errors that were caused due to the effect of label biomolecule on the binding of biomolecule [5]. Smartphones can also be used for lable-free biodetection [6].

Among the label-free sensor, a surface plasmon resonance sensor has gained huge attraction for characterizing and determiningbiomolecular interaction without the use of labelledbiosensors [7]. Optical biosensors made from surface plasmon resonance can determine any complexity of biomolecule from micro to macromolecule such as receptor-ligand interaction [8], [9]. Real-time biomolecular interactions can be possible through labelled free biosensors using surface plasmon resonance [10]. SPR sensors are independent of excitations of plasmons and modulation methods such as amplitude, wavelength,etc. and depend only on the properties of light that are used in detectors. They use the surface plasmon resonance that can detect the minor range of refractive index [11]. Plasmonic structure advances in developing the modern biosensor which allows the high intensity of light intensity of sub-wavelength to be constructed in micrometer range that can be integrated with small chips also [12]. A gold metasurface array biosensor is used for achieving higher sensitivity for different hemoglobin biomolecules [13]. Grating waveguide biosensor is used to improve the sensitivity for hemoglobin biomolecules [14]. Fibre-optic surface plasmon resonance sensor advances a lot in the field of research [15]. They can be designed as per the requirement of geometry shapes they can deal with electrical noise, high voltage, and temperature, corrosiveness from where the sensing layer is generated for different layers, etc., [16]. Graphene perturbations are added in waveguide to create leaky-wave behaviour which helps in sensing blood plasma biomolecules [17]. Bragg gratings resonator is used for sensing biomolecules and increasing its sensitivity [18], [19]. The optical biosensor is based onthe diagnosis of pathogens that are the main causes of infectious diseasesthat result sometimesindeath also. The biosensor has advanced the research and its development using a plasmonic biosensor. Among the most commonly used is SPR biosensor due to the

advancement in nanotechnology it makes them easy to use, cost-effective, miniature, and fully integrated biosensor that is as useful in environmental monitoring, clinical amplifications, forensics, food safety,defence,etc. [20], [21]. Surface plasmon resonance is the most common technique of optical sensor used. Its main application is to observe the change in the refractive index that is occurring near the surface of the sensor that is responsible for increased sensitivity. They are used for early detection of the many viruses that are harmful to humansand can be easily be diagnosed [22]. They are useful for food safety for detecting and maintaining hygiene purposes. Food acts as a growth medium for microorganisms that is responsible for spoiling the food or giving rise to harmful bacteria, viruses, etc., [23]. Metasurface based biosensor with graphene material can be used to increase sensitivity [24]. Urinary tract infections can be tracked using surface plasmon resonance-based biosensor [25–27].

Phase changing materials are gaining interest because of their tuning behaviour [28–31]. Phase change material can be used to improve cooling and efficiency [29]. Phase change material also showing transparency and broadband behaviour [30]. Phase change materials store the data information in both the phases crystalline and amorphous which can be controlled by an external voltage [32]. The change and combination of electronic and optical properties thatthey maintain provide the high and low resistivity between amorphous a crystalline phases [33]. These phase change materials possess good conductivities that result in good efficiency which is useful in many applications of solar, sensor, etc. [34–37].

The biosensors presented so far in the literature clearly show that an improvement in sensitivity can be achieved. Tunability is another important which is required for sensitive biosensors. Here we propose tunable and highly sensitive biosensors using GST material. The amorphous and crystalline phases of GST material are used to achieve tuning of spectrum. The high sensitivity is also achieved and compared with previously published similar designs to show the improvement. The electric and magnetic field results are also analyzed. The biosensor metasurface design is presented in Section 2. The absorption results for both phases and different hemoglobin concentrations are presented in Section 3. The conclusion is presented in Section 4.

2. Design and modelling

The metasurface biosensor design based on GST material is presented in Fig. 1. The gold metasurface of 0.3 μm is placed above GST substrate having a thickness 0.6 μm. The gold ground plane is of 0.3 μm thickness. The biomolecules are placed above the gold metasurface layer as presented in Fig. 1(a) which shows the front view of the design in 2D form. The top view of the design and 3D view of the design is presented in Fig. 1(b) and Fig. 1(c) respectively.
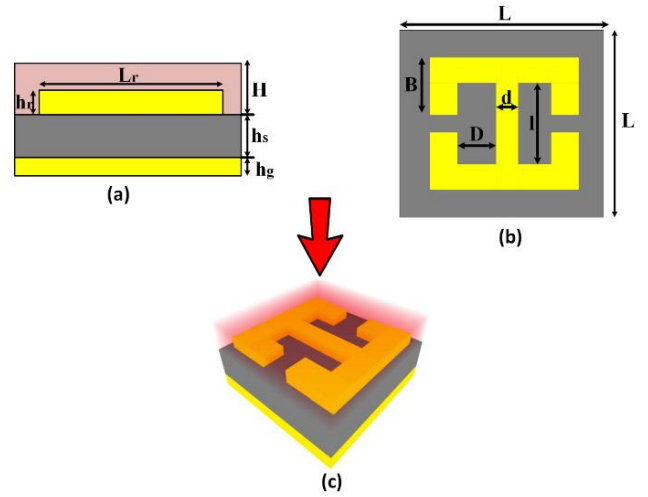

Fig. 1. GST based metasurface biosensor design (a) 2D front view (b) 2D top view and (c) 3D view. The different dimensions Lr, hr, H, hs, hg, B, d, l, D, L are given by 3 μm, 0.3 μm, 0.6 μm, 0.6 μm, 0.3 μm, 1.3 μm, 0.5 μm, 2 μm, 0.75 μm, 3.5 μm respectively. The grey color material is GST material. Yellow color material is gold material. The arrow indicates the light falling onto the sensor. Biomolecules are placed above gold metasurface resonator (color online)

Metasurface analysis:

Metasurface analysis is very important for this design and permittivity and permeability are two important parameters for the metasurface analysis. These two parameters can be calculated from the reflection coefficient and transmission coefficient as shown in the following equations (1-5). The S$_{11}$ is the reflectance and S$_{21}$ is the transmittance. Both these parameters are calculated from simulation environment and added in the equation to calculated metasurface parameters permittivity and permeability. A detailed analysis of the metasurface can be obtained from [38]:

$$z = \pm \sqrt{\frac{(1+S_{11})^2 - S_{21}^2}{(1-S_{11})^2 - S_{21}^2}} \qquad (1)$$

$$e^{ink_0 d} = \frac{S_{21}}{1 - S_{11}\frac{z-1}{z+1}} \qquad (2)$$

$$n = \frac{1}{k_0 d}[\{[\ln e^{ink_0 d}]'' + 2m\pi\}] - i[\ln(e^{ink_0 d})]'] \quad (3)$$

$$\varepsilon = \frac{n}{z} \qquad (4)$$

$$\mu = n\,z \qquad (5)$$

Sensitivity analysis:

The sensitivity is calculated from wavelength peak difference for different refractive index biomolecules and presented by [39]:

$$S = \frac{\Delta\lambda}{\Delta n} \qquad (6)$$

3. Results and discussions

The GST based metasurface biosensor design presented in Fig. 1 is analyzed using COMSOL Multyphysics with finite element method (FEM). The Delaunay triangular meshing is used in this research with minimum element size of 2 nm. Periodic boundary conditions are used in this research. The results in the form of absorption, electric field, angle variation, and different geometrical parameter variation are presented in Fig. (2-8). The absorption results for aGST and cGST are presented in Fig. (2-4) and the comparative plot is presented in Fig. 5. The design results are carried out for four different haemoglobin biomolecules concentrations having refractive index 1.34 (10g/l), 1.36 (20g/l), 1.39 (30g/l) and 1.43 (40g/l). The results are observed for the range of 0.6 µm to 1 µm wavelength range. The aGST absorption results presented in Fig. 2 are for four different concentrationsthat clearly show the wavelength peak variation between them. The peak wavelengths are achieved between 0.73 µm to 0.78 µm for different hemoglobin concentrations.
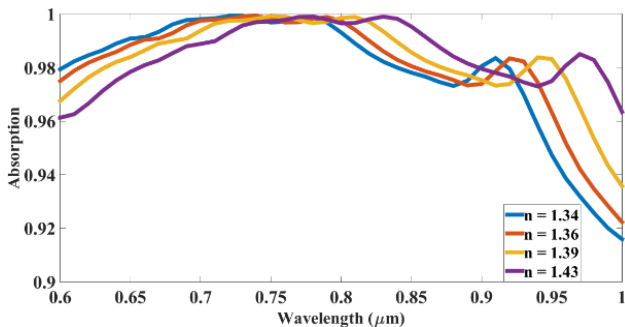
The cGST absorption results presented in Fig. 3 are for four different concentrationsthat clearly show the wavelength peak variation between them. The peak wavelengths are achieved between 0.68 µm to 0.73 µm for different hemoglobin concentrations. The comparison of aGST and cGST for 1.34 refractive index hemoglobin biomolecule concentrations is presented in Fig. 4. The comparison clearly shows the shift between the peak wavelengths. The peak wavelength for cGST and aGSTis 0.68 µm and 0.73 µm. The tenability of 50 nm is achieved using these two different phases of GST material. The GST material is the most suitable for tunablebiosensing because the change in phase of GST material shifts the spectrum of the biosensor. The phase shift also changes the overall absorption of the spectrum. Because of these reasons GST material is used in this research.

The comparison of aGST results and cGST results for all the hemoglobin concentrations are presented in Table 1. The sensitivity is calculated from the wavelength difference and refractive index difference as given by equation (6). The maximum sensitivity for aGST and cGST is 750 nm/RIU and 900 nm/RIU.

Table 1. Sensitivity analysis aGST and cGST results for different hemoglobin concentrations

		n_1	n_2	n_3	n_4
		1.34	1.36	1.39	1.43
	Δn	0.02	0.03	0.04	
aGST	λ (µm)	0.73	0.74	0.75	0.78
	$\Delta\lambda$ (nm)	10	20	20	
	S(nm/RIU)	500	666	**750**	
cGST	λ (µm)	0.682	0.70	0.71	0.73
	$\Delta\lambda$ (nm)	20	20	20	
	S(nm/RIU)	**900**	250	500	

Fig. 2. Absorption results for aGST phase for different hemoglobin biomolecules concentrations. The peak wavelengths are 0.73 µm, 0.74 µm, 0.75 µm, 0.78 µm for haemoglobin concentrations with refractive index values 1.34, 1.36, 1.39 and 1.43 respectively (color online)
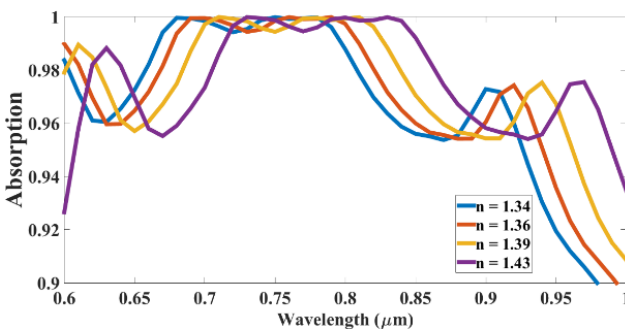

Fig. 3. Absorption results for cGST phase for different hemoglobin biomolecules concentrations. The peak wavelengths are 0.682 µm, 0.70 µm, 0.71 µm, 0.73 µm for haemoglobin concentrations with refractive index values 1.34, 1.36, 1.39 and 1.43 respectively (color online)
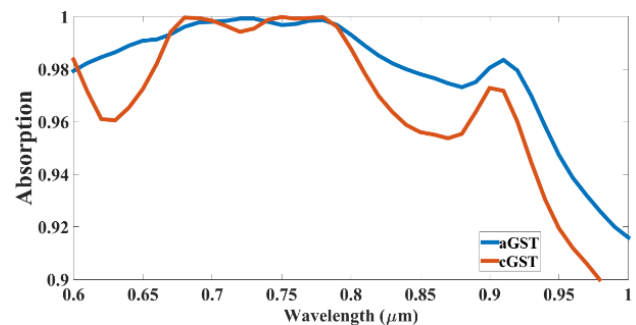

Fig. 4. Comparative plot aGST and cGST absorption results for hemoglobin biomolecules with refractive index 1.34. The absorption difference is visible between the two phases (color online)
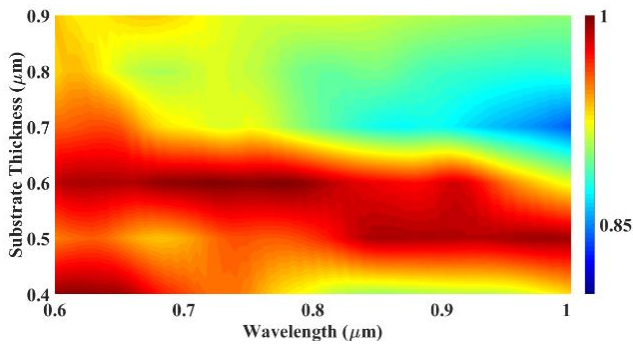
Fig. 5. GST based metasurface based biosensor design absorption result for different substrate thickness. The thickness is varied from 0.4 μm to 0.9 μm. The maximum absorptionresults are visible at 0.6 μm substrate thickness (color online)

The different geometric parameters of the design like substrate thickness and resonator thickness are varied for aGST phase to observe its effect on the absorption results and presented in Figs. 5-6. The absorption results for substrate thickness of 0.4 μm to 0.9 μm is presented in Fig. 5. The substrate thickness is very important as it absorbs most of the light that falls on the design. The substrate thickness of 0.6 μm is showing the maximum absorption for the biosensor design.
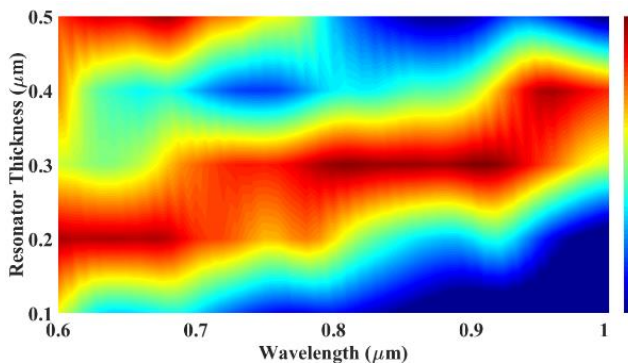

Fig. 6. GST based metasurface based biosensor design absorption result for different resonator thickness. The thickness is varied from 0.1 μm to 0.6 μm. The maximum absorption results are visible around 0.3 μm resonator thickness (color online)

The variation in absorption results for different metasurface thickness is presented in Fig. 6. The metasurface thickness is increased to a high level than resonance is affected and absorption is shifted as visible in the figure. As we increase the resonator thickness the absorption bands are shifting and the best results are visible around 0.3 μm thickness. The red color shows the maximum absorption which is visible more in middle thicknesses for the whole range. The absorption peak is shifting for different values of resonator thickness.
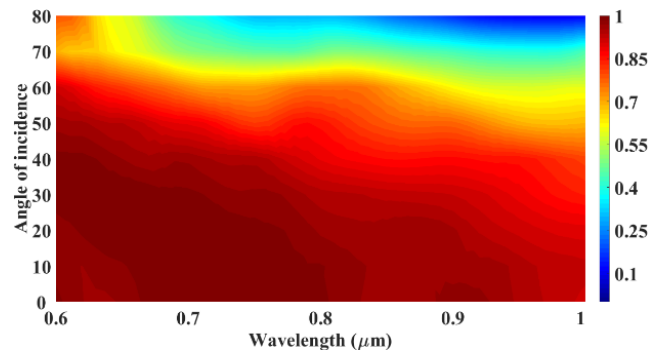

Fig. 7. GST based metasurface based biosensor design absorption result for different angle variation. The angle is varied 0° to 80°. The angle results are giving better absorption for lower angles and as angleincreases the absorption reduces (color online)

The incident angle play important role in biosensing. The angle of incidence is varied from 0° to 80°. The absorption results are presented in Fig. 7 for all the angle variations. The absorption results are more than 80% for initial angles of 0° to 60°. The results are degrading as we increase the angle further as shown in the figure. The absorption is decreased for 70° and 80° angles which are visible in the figure. The electric field and magnetic field results for three different wavelengths 0.65 μm, 0.75 μm, and 0.85 μm is presented in Fig. 8. All three results show absorption and current in the figures as they have more than 80% absorption for all these three wavelengths as presented in the line plot of Fig. 2. The electric field and magnetic field results are justified the same. The maximum absorption is visible around 0.75 μm wavelength results. The electric field intensity is differentiated by different colors where blue color shows the minimum value and red color shows the maximum value.
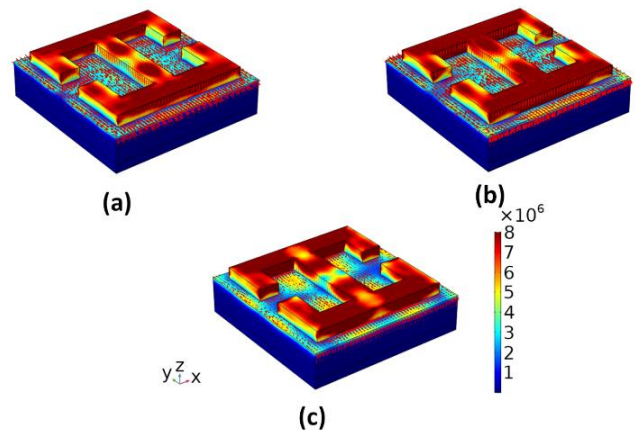

Fig. 8. Electric field and magnetic field current results for the GST based metasurface biosensor design for (a) 0.65 μm (b) 0.75 μm and (c) 0.85 μm. The maximum absorption and current is visible around 0.75 μm

The proposed GST based metasurface biosensor design is compared with a previously published similar design and the comparison is provided in Table 2. From the comparison, it is clear that the proposed design has better sensitivity compared to the other designs. The crystalline phase of GST based biosensor is giving the best sensitivity of 900 nm/RIU.

Table 2. Sensitivity comparison of the proposed design with previously published designs

Design	Sensitivity (nm/RIU)
Proposed biosensor with aGST	750
Proposed biosensor with cGST	900
Biosensor for sensing hemoglobin from [14]	322
Biosensor for sensing hemoglobin from [18]	387
Biosensor sensing hemoglobin from [27]	500

4. Conclusion

The GST based metasurface biosensor design for sensing hemoglobin biomolecules is presented. The results are analyzed for absorption for different hemoglobin concentrations. The sensitivity is calculated from the wavelength peak difference and refractive index difference. The amorphous GST phase has the highest sensitivity of 750 nm/RIU and the crystalline GST phase 900 nm/RIU. The geometrical parameter thickness is varied to check its performance on absorption. The best substrate thickness and metasurface thicknesses are 0.6 µm and 0.3 µm. The angle of incidence is also varied to check its effect of absorption. The results show that it is angle sensitive and gives better results for lower angles. The absorption result is better for a lower angle of incidence. The design results comparison with previously published results shows improvement in the proposed design. The proposed optical biosensor is applicable in medical sensing applications.

References

[1] N. Gu, S. Liu, Journal of Materials Chemistry B **8**(16), 3168 (2020).

[2] K. N. Shushama, M. M. Rana, R. Inum, M. B. Hossain, Opt. Quantum Electron. **49**, article number 381 (2017).

[3] J. S. Daniels, N. Pourmand, Electroanalysis **19**(12), 1239 (2007).

[4] G. Zanchetta, R. Lanfranco, F. Giavazzi, T. Bellini, M. Buscaglia, Nanophotonics **6**(4), 627 (2017).

[5] N. Khansili, G. Rattu, P. M. Krishna, Sensors and Actuators B: Chemical **265**, 35 (2018).

[6] D. Gallegos, Hojeong Yu, Peter P. Clark, Yixiao Lin, Sherine George, Pabitra Nath, Brian T. Cunningham, Lab Chip **13**(11), 2124 (2013).

[7] J. Homola, S. S. Yee, G. Gauglitz, Sensors Actuators B Chem. **54**(1), 3 (1999).

[8] P. Pattnaik, Applied Biochemistry and Biotechnology **126**(2), 79 (2005).

[9] J. Homola, M. Piliarik, "Surface Plasmon Resonance (SPR) Sensors," Springer, Berlin, Heidelberg **45** (2006).

[10] B. Liedberg, C. Nylander, I. Lundström, Biosens. Bioelectron. **10**(8), i–ix (1995).

[11] M. Piliarik, J. Homola, Opt. Express **17**(19), 16505 (2009).

[12] A. G. Brolo, Nature Photonics **6**(11), 709 (2012).

[13] S. K. Patel, J. Parmar, H. Trivedi, R. Zakaria, T. K. Nguyen, V. Dhasarathan, IEEE Photonics Technol. Lett. **32**(12), 681 (2020).

[14] S. Sahu, J. Ali, P. P. Yupapin, G. Singh, Optik **166**, 103 (2018).

[15] A. K. Sharma, R. Jha, B. D. Gupta, IEEE Sensors Journal **7**(8), 1118 (2007).

[16] T. G. Giallorenzi, J. A. Bucaro, A. Dandridge IEEE Trans. Microw. Theory Tech. **30**(4), 472 (1982).

[17] S. K. Patel, J. Parmar, Y. P. Kosta, M. Ladumor, Sensors Actuators, A Phys. **301**, 111767 (2020).

[18] S. Sahu, J. Ali, P. P. Yupapin, G. Singh, Photonic Sensors **8**, 248 (2018).

[19] S. K. Patel, S. Charola, J. Parmar, M. Ladumor, Q. M. Ngo, V. Dhasarathan, Opt. Quantum Electron. **52**(5), 1 (2020).

[20] S. M. Yoo, S. Y. Lee, Trends in Biotechnology **34**(1), 7 (2016).

[21] S. Patel, J. Parmar, D. Katrodiya, T. K. Nguyen, E. Holdengreber, Vigneswaran Dhasarathan, J. Opt. Soc. Am. B **37**(7), 2163 (2020).

[22] P. Jahanshahi, E. Zalnezhad, S. D. Sekaran, F. R. M. Adikan, Sci. Rep. **4**(1), 1 (2014).

[23] K. Narsaiah, S. N. Jha, R. Bhardwaj, R. Sharma, R. Kumar, Journal of Food Science and Technology **49**(4), 383 (2012).

[24] S. K. Patel, J. Parmar, Y. P. Kosta, S. Charola, IEEE Sens. J. **20**(12), 6359 (2020).

[25] E. Özgür, A. A. Topçu, E. Yılmaz, A. Denizli, Talanta **212**, 120778 (2020).

[26] L. Lu, L. T. Chew, R. E. Simpson, T. Cao, W. Dong, X. Zhou, OPJ-OSA Jt. Symp. Nanophotonics Digit. Photonics (2017), Pap. 31aON1, 31aON1 (2017).

[27] Shobhit K. Patel, Juveriya Parmar, Rozalina Zakaria, A Sharafali, Truong Khang Nguyen, Vigneswaran Dhaasarathan, IEEE Sens. J. **21**(2), 1470 (2020).

[28] H. Tao, W. J. Padilla, X. Zhang, R. D. Averitt, IEEE J. Sel. Top. Quantum Electron. **17**(1), 92 (2011).

[29] M. S. B. Pruthvi, G. Viswanath, Mater. Today Proc. **33**, 559 (2020).

[30] Y. Zhang, Junying Li, Jeffrey Chou, Zhuoran Fang, Anupama Yadav, Hongtao Lin, Qingyang Du, Jerome Michon, Zhaohong Han, Yizhong Huang, Hanyu Zheng, Tian Gu, Vladimir Liberman,

Kathleen Richardson, Juejun Hu, Conference on Lasers and Electro-Optics, CLEO 2017 - Proceedings **2017**, 1 (2017).

[31] D. Ielmini, A. L. Lacaita, A. Pirovano, F. Pellizzer, R. Bez, IEEE Electron Device Lett. **25**(7), 507 (2004).

[32] S. Raoux, F. Xiong, M. Wuttig, E. Pop, MRS Bull. **39**(8), 703 (2014).

[33] H.-S. Philip Wong, Simone Raoux, Sang Bum Kim, Jiale Liang, John P. Reifenberg, Bipin., Proceedings of the IEEE **98**(12), 2201(2010).

[34] A. K. Bhargava, Appl. Energy **14**(3), 197 (1983).

[35] S. Raoux, Wuttig, Matthias, Proceedings -2007 Non-Volatile Memory Technology Symposium, NVMTS 07, **2007**, 30 (2007).

[36] M. Nejat, N. Nozhat, J. Phys. D. Appl. Phys. **53**(24), 245105 (2020).

[37] Z. Guo, X. Yang, F. Shen, Q. Zhou, J. Gao, K. Guo, Sci. Rep. **8**, 12433 (2018).

[38] A. B. Numan, M. S. Sharawi, IEEE Antennas Propag. Mag. **55**(5), 202 (2013)

[39] A. Dolatabady, S. Asgari, N. Granpayeh, IEEE Sens. J. **18**(2), 569 (2018).

_____
[*]Corresponding author: sdmustafa88@gmail.com